In this article, we report the observation of an air-encapsulating elastic mechanism of Dandelion spherical seed heads, namely blowballs, when submerged underwater. This peculiarity seems to be fortuitous since Taraxacum is living outside water; nevertheless, it could become beneficial for a better survival under critical conditions, e.g. of temporary flooding. The scaling of the volume of the air entrapped suggests its fractal nature with a dimension of 2.782 and a fractal air volume fraction of– 4.82 10^2 $m^{0.218}$, resulting in nominal air volume fractions in the range of 14 23%. This aspect is essential for the optimal design of bioinspired materials made up of Dandelionlike components. The miniaturization of such components leads to an increase in the efficiency of the air encapsulation up to the threshold (efficiency ¼ 1) achieved for an optimal critical size. Thus, the optimal design is accomplished using small elements, with the optimal size, rather than using larger elements in a lower number. The described phenomenon, interesting per se, also brings bioinspired insights toward new related technological solutions for underwater air-trapping and air-bubbles transportation, e.g. the body surface of a man could allow an apnea (air consumption of 5¯10 l/min) of about 10 min if it is covered by a material made up of a periodic repetition of Dandelion components of diameter ffi18 μm and having a total thickness of about 3¯6 cm.

1. Introduction

The ability of nature to show sophisticated features has stimulated the researchers ¯ starting from the Italian Renaissance genius Leonardo da Vinci ¯ toward the realization of innovative bioinspired devices [1,2]. For instance, animals show very efficient compliant mechanisms to move in the air, water, and/or on the ground, giving rise to new research fields, for instance, soft-robotics [3,4], e.g. in underwater propulsion [5] or actuators [6¯9]. Natural organisms are known for their complex hierarchical from nano- to macro-sized architectures that allow them the achievement of extreme physical and mechanical characteristics, both in static and in dynamic regimes. The hierarchy of the microstructure also plays a crucial role in peeling and adhesion phenomena [10¯12]. For instance, the feet of geckoes are covered with elastic hairs whose ends split into nanoscale structures, called spatula: such a hierarchical microstructure allows them to adhere to almost any type of material [13¯15]. Another intriguing property of living organisms concerns the water-air-solid interaction, e.g. the super hydrophobicity of surfaces of certain plant leaves, mainly because of its wide range of application and cross-disciplinary interest, e.g. self-cleaning surfaces. This phenomenon, known as 'lotus-effect', is observed in nature both in plants and animals [16¯18]. By contrast, hydrophilicity and surface charge are responsible for attracting water and the folding propensity of a membrane [19,20]. Within this framework, an important role is played by underwater air-retaining surfaces because of their technological high-impact. In nature, there are some examples of plants and animals that developed a peculiar air-retaining mechanism depending on their specific purpose. Some insects and spiders (diving bugs, beetles, and spiders) that spend most of their lives underwater developed peculiar air-retaining mechanisms. These species can survive for a long time in the water because of an air-store bubble that acts as a physical gill to obtain dissolved O_2 from the water [21].

For instance, diving bell spider or water spider [22], a species that lives mostly underwater, developed ingenious air-encapsulating mechanisms. This spider can survive for a long time in the water, although it breathes air because of a clever silk-based microstructure allowing the storage of oxygen supply. Such a structure, called the diving bell, is made up of hydrophobic hairs that permit the trapping of air-filled bubble on its abdomen and legs by giving them a silvery coloring. The diving bell works as a physical gill, where the air remains trapped by the surface tension between the silk-fibers of their underwater web [23,24].

A different mechanism for long-term air-retention underwater is exhibited by the floating water fern Salvinia Molesta. In particular, the work by Barthlott et al. [25] showed that the sophisticated microstructure of Salvinia, when dived in the water, combines high-hydrophobicity and hydrophilicity to create a very efficient yet elegant air-retaining mechanism. In this case, the air-water interface is due to the eggbeater shape of the leaves and the presence on the surface of hydrophilic tips that prevent its failure [26¯28]. Accordingly, several studies focused on the artificial replication of the Salvinia leaf [29¯37].

In the present article, we show that also Dandelion ripe seed heads ('fluffy ball' composed of seeds with pappus parachute fluff), show a very efficient compliant mechanism to retain air underwater. Dandelions are not new to exhibit peculiar behaviors. The passive flight mechanism of dandelion seeds drawn the attention of researchers because of its high effective; recently, Cummins et al. [38] conducted a detailed study on the physics behind such a mechanism: they visualized the flow around dandelion seeds discovering a peculiar type of vortex. Our present study concerns the analysis of an efficient Dandelion air-retaining mechanism underwater, as shown in Fig. 1, outside its usual living condition that however could have a role under critical condition, e.g. for surviving to temporary flooding. In the literature, there are examples of bioinspired air retaining mechanisms, but they are based on different working principles. The mechanism presented in the article is a complaint mechanism that represents a very sophisticated way for air-trapping.

Fig. 2 shows the working principle of such a mechanism. The hydrophilic bristles (the pappus) close elastically encapsulating a small water droplet [39¯41]. Different confined water droplets of the different bristles connect each other again thanks to elastic compliance of the structure and doing so create a water wall able to retain air when the seed head is submerged. It is interesting to notice that the mechanism is reversible. The mechanism is fully or partially reversible depending on the time that elapses between when the seed head is removed from the water and it is submerged again. For an almost 'instantaneous' re-immersion the mechanism is partially reversible since the seeds remain partially wet when the flower is removed from the water and the subsequent air encapsulation is less efficient. For a time long enough to dry the seeds completely, the mechanism becomes fully reversible and the seed heads returns to its initial shape. Concerning the elastic mechanism, it is clear that the seeds are loosely fixed on the stem, but such mechanical fuse is designed to release the seeds only when the proper dispersion period and environmental conditions are reached. Thus, our experiments were conducted before that period and the same flowers resist for several repetitions. Even natural flowers can thus be sufficiently strong and artificial bioinspired solutions are expected to be much stronger, even just simply removing the mechanical fuse present in nature. The little umbrellas at the top of each seed heads are made up of a cluster of thin hydrophilic hairs. We have observed that as soon the hairs make contact with water, they instantaneously close trapping a water droplet. Then, each seed head connects with those nearby to create a thin air-retaining surface. Therefore, the little umbrellas' complaint nature combined with the hydrophilic hairs generates a very thin water film able to trap a non-negligible volume of air inside.

A video showing the reversible air-trapping compliant mechanism is available as supplementary material. This study provides a clear evidence of a potential new way of thinking about bioinspired materials with respect to the bioinspired air-trapping mechanisms already present in the literature. In particular, the compliant mechanism discussed in the article brings new bioinspired insights towards new related technological solutions for underwater air-trapping and air-bubbles transportation.

2. Analytical model and experimental protocol

A specific procedure, schematically shown in Fig. 3, was developed and used in the experiments to estimate the volume of the air, V_{air}, encapsulated from the Dandelion seed heads when dived in the water. First, both the weight of the whole Dandelion clock (seed heads þ stem), W_{tot}, and diameter of the seed head, $D_{seed\text{-}heads,dry}$, were measured (Fig. 3(a)). Then, the Dandelion clock was dived into a water tank (Fig. 3(b)). In so doing, each of the little umbrellas at the top of the seeds closes forming a thin water film trapping a non-negligible volume of air inside.

The upward floating reaction force, R_{tot}, measured at the load cell, is equal to the difference between the buoyant force $F_{B,tot}$ and the weight of the Dandelion clock W_{tot}

$$R_{tot} = F_{B;tot} - W_{tot} = \rho_w g V_{stem} + V_{seeds} + V_{air} g \rho_{stem} V_{stem} + \rho_{seed} V_{seeds} : \quad (1)$$

The same procedure was repeated to determine the floating force provided by the stem (Fig. 3(c)) defined as

$$R_{stem} = F_{B;stem} - W_{stem} = \rho_w g V_{stem} \rho_{stem} g V_{stem} : \quad (2)$$

Finally, the stem was weighted (Fig. 3(d)) to determine, indirectly, the weight of the seeds, W_{seeds}, through the relation

$$W_{seeds} = W_{tot} - W_{stem} = g \rho_{seed} V_{seeds} : \quad (3)$$

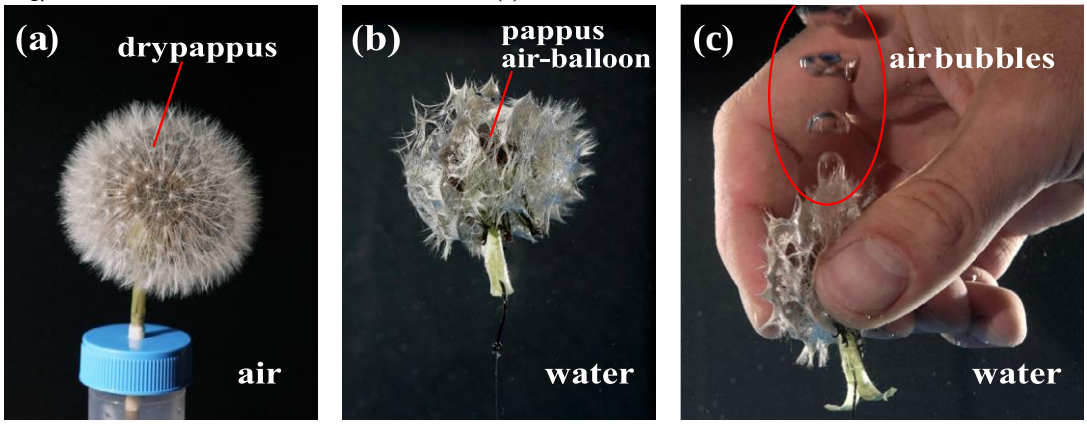

Fig. 1. Example of a Dandelion ripe seed heads (fluffy ball) before the immersion in the water (a) and when dived in the water (b). In the latter case, the little umbrellas at the top of each pappus close encapsulating a non-negligible volume of water. All the wet umbrellas create a barrier to additional water forming a kind of balloon containing air. Such air causes an up-thrust, as can be noted observing the tensioned fishing wire. (c) A seeds balloon is squeezed. The air entrapped inside the balloon comes out in the form of bubbles rising to the top of the tank.

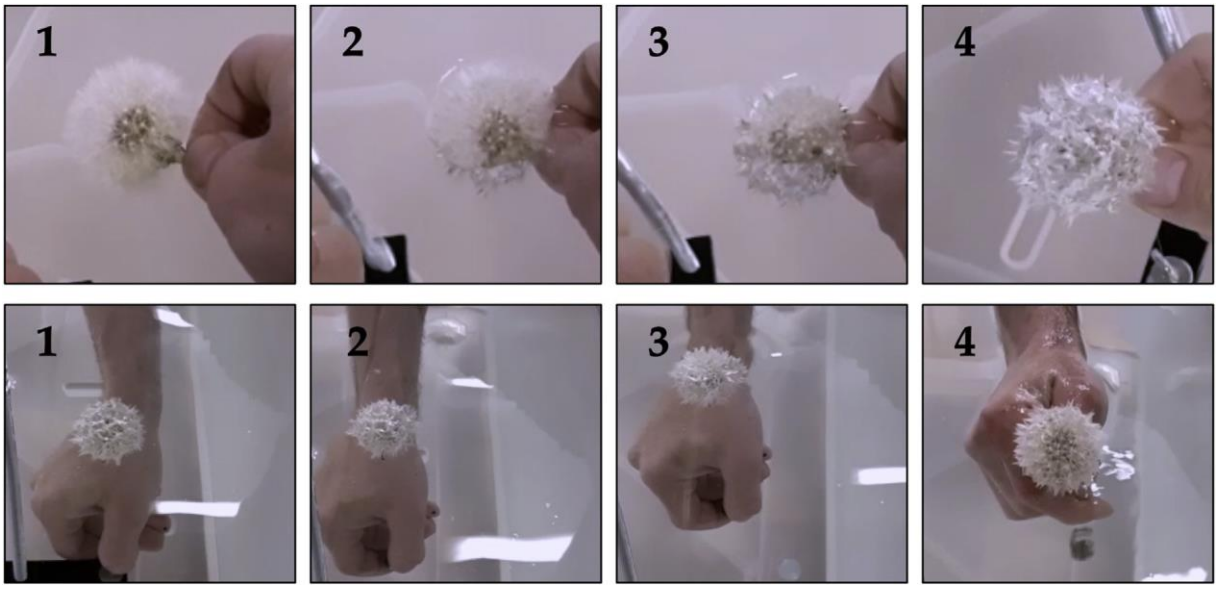

Fig. 2. Snapshots extracted from a movie, taken during an experiment, to show the air-trapping mechanism of the Dandelion composite seed heads. (top) The seed heads is dived in water. The hydrophilic seeds close and create a very thin air-retaining hydrophobic surface. (bottom) The seed heads is removed from the water revealing the reversibility of the air-trapping mechanism.

The buoyant force generated by the air encapsulated inside the seeds balloon can be easily computed noting that the difference between the reaction forces mentioned above, both measured in the experiments, reads

$$\Delta R_B = R_{B;tot} - R_{B;stem} = \rho_w g \forall V_{seeds} + V_{air} + g \rho_{seed} V_{seeds}: \quad (4)$$

Under the reasonable assumptions that $V_{seeds} \ll V_{air}$, the up-thrust, $F_{B;air}$, due to the air trapped within the seeds balloon can be approximatively estimated as

$$F_{B;air} = g \rho_w V_{air} \text{ ffi } \Delta R_B + W_{seeds}: \quad (5)$$

By inverting the previous equation, it is trivial to determine the corresponding volume of the air trapped within the seeds balloon

$$V_{air} = \frac{F_{B;air}}{\rho_w g}: \quad (6)$$

With a view to make the encapsulated air in terms of volumetric content, it is convenient to introduce the dimensionless quantity

$$\overline{V}_{air} = \frac{V_{air}}{V_{seedheads;dry}}; \quad (7)$$

where $V_{seed\text{-}heads,dry}$ represents the nominal volume of the seed head prior the immersion in water.

The experiments were performed exploiting the experimental setup shown in Fig. 4.

A glass tank, filled by water, is used to capture the charming airencapsulating mechanism of the Dandelion seed head when immersed in water. The floating force was measured through a load cell (Lean DBBSM RC 10N) mounted on a rigid aluminum frame. The weight of the seed head and stems were measured using an Orma EB 200 scale, sensitivity 0.0001 g. After being weighted, both the seed heads and the stems were dived in the tank.

The Dandelion is hooked via a magnetic clip to a black PMMA support. Such a basement is connected to the load cell with a metal stinger, as shown in Fig. 4, realizing, for the involved forces, a rigid cantilever beam. The floating force was measured through a load cell (Lean DBBSM RC 10N) mounted on a rigid aluminum frame out of the tank. At

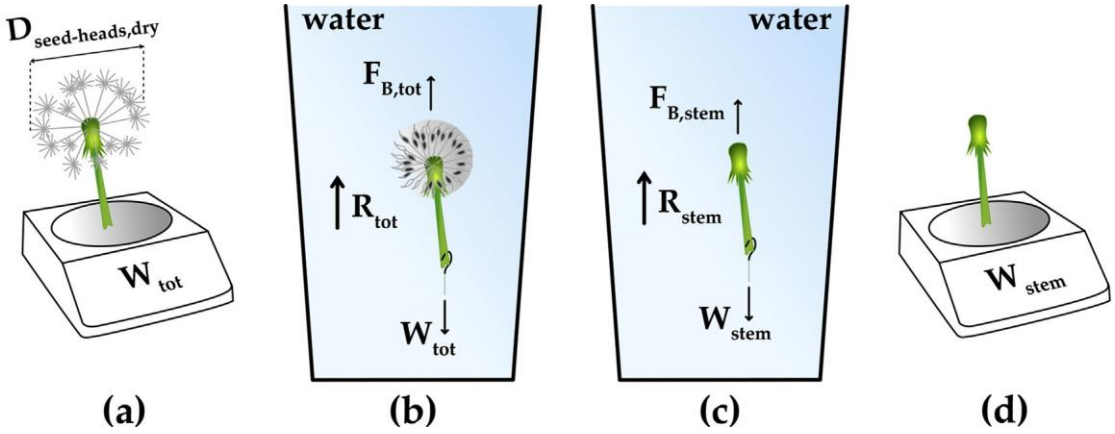

Fig. 3. Schematization of the experimental protocol followed to determine the air volume encapsulated within the pappus balloon generated when the seed heads is dived in the water. (a) First, the Dandelion clock (stem and seeds) is weighted, and the dry diameter of the seed heads is measured. (b) The Dandelion clock is dived into a water tank, and the buoyant force R_{tot} is measured. (c) The buoyant force for the stem R_{stem} is also measured. (d) Finally, the stem is weighted.

Fig. 4. A photograph of the experimental setup used to measure up-thrust provided by the encapsulated air.

beginning of each weighing session, the load cell (hanging the metal stinger, the magnetic clip, the hook used to attach the seed heads and the black PMMA support) was tared to zero. Therefore, the weights of the suspended objects are irrelevant to the procedure and the loads measured by the load cell are precisely the wanted buoyant forces R_{tot} and R_{stem}.

Alongside the execution of the experiment, pictures were taken with a Sony alpha9 camera and movies with a Sony PXW FS-5 high-speed camera. The Dandelion clocks used in the experiments were collected all in the same meadow located near our University. The proposed experiments, that at first sight could seem easy, were quite challenging and required several repetitions. The success of the tests was strictly connected with the temperature (or better the daily temperature variation) experienced by the flower in the two/three days before the opening of the seeds balloon. In fact, the mechanical fuse of the flower is designed to release the seeds only when the proper dispersion period and environmental conditions are reached. Thus, our experiments were conducted before that period and the same seed head resists for several repetitions. 3. Results and discussion

Following the experimental-analytical approach discussed in the previous section, several experiments were performed to estimate the volume of the air entrapped in the seeds balloon. All the results are collected in Table 1 and show that the average dimensionless volume,

$\overline{V}_{air}$, of the air encapsulated by the air-trapping mechanism is equal to 0:185 0:026. This value corresponds to a buoyant force of about 105:043 28:22 mN.

In Fig. 5, the air trapped by the submerged seed head is plotted as a function of its diameter (before its immersion in the water). The result

Table 1

shows that the volume of the air scales as $V_{air} \propto fD_{seedheads;dry}^{\alpha}$ (purple/ dashed line), where the exponent $\alpha \approx 2.782$ is the fractal dimension of the air-entrapping domain, in contrast to the classical Euclidean scaling law dimension of 3 (dashed/blue line) and $f \approx 4.82 \cdot 10^{2}\ m^{0.218}$ is a constant prefactor with anomalous physical units representing the fractal air-entrapped volumetric content. In the same Figure it is also reported the scaling law dimension of 2 (dashed-dotted/green line). In particular, a scaling law with a characteristic dimension lower than 3 implies that the percentage of the entrapped volume of air is not constant but depends on the nominal size of the seed head. This aspect plays a crucial role in the optimal design of bioinspired materials made up of Dandelion-like components. The lower is the characteristic dimension of the basic component, the higher is the efficiency of the resultant material in terms of encapsulated volume fraction. Of course, this efficiency reaches the threshold value of 1 for a critical size, namely

$$D_{seedheads;optimal} \approx \left(\frac{f}{\pi}\right)^{\frac{1}{3-\alpha}} \quad (8)$$

For dimension lower than $D_{seedheads;optimal}$ the efficiency remains maximal.

Thus, thinking to the optimal design of Dandelion-like bioinspired materials or devices it is convenient, for simultaneously maximizing air trapping and minimizing used material/weight/cost, increasing the number of elements with the size reported in eq. (8), rather than using larger elements in a lower number (less efficiency) or vice-versa (more weight). This scaling is understandable, considering the example shown in Fig. 5(c and d). The same volume is filled with just 1 seed head (diameter $D_1 \approx L$) in Fig. 5(c) or with n^3 smaller seed heads (diameter $D_n \approx L/n$) in Fig. 5(d).

The volume of the air entrapped using 1 seed head or n^3 seed heads (with the same total volume) is equal to $V_{1;air} \propto f L^{\alpha}$ or $V_{n^3;airD\ splitting} \propto f \frac{L^{\alpha}}{n^3}$, respectively. Taking the ratio between these values we end up with the relation

$$\frac{V_{n^3;airD\ splitting}}{V_{1;air}} \approx n^{3-\alpha} \quad (9)$$

For a number of components $n > 1$ and an exponent $\alpha < 3$ the righthand side term in eq. (9) is higher than 1. This result proves mathematically that the splitting — the use of more miniaturized components — leads to a higher volume of the entrapped air. This is true up to the physical threshold defined by eq. (8).

To give comparative goodness of fit analysis in predicting the observed data, we computed the root mean square error (RMSE), defined as

$$RMSE = \sqrt{\frac{\sum_{i}^{m} (y_i - y_{fit})^2}{m}} \quad (10)$$

Experimental results. For each seed head, the volume of the air entrapped inside the balloon is determined.

Sample	$D_{seed\ heads;dry}$ [cm]	$V_{seed\ heads;dry}$ [cm^3]	W_{tot} [mN]	W_{stem} [mN]	W_{seeds} [mN]	R_{tot} [mN]	R_{stem} [mN]	$F_{B;air}$ [mN]	V_{air} [cm^3]	$\overline{V}_{air}$ [ ]
1	5.324	79.02	9.7334	6.7189	3.0145	301.13	141.04	163.10	16.63	0.210
2	4.671	53.36	7.3814	5.2146	2.1668	222.07	123.03	101.20	10.32	0.193
3	4.706	54.57	5.3234	2.5656	2.7577	184.67	102.97	84.46	8.61	0.158
4	4.729	55.37	4.2816	1.7758	2.5059	181.65	84.67	99.49	10.14	0.183
5	5.622	93.04	7.2461	4.1366	3.1095	236.88	113.88	126.11	12.86	0.138
6	4.503	47.81	6.8453	4.1513	2.6940	182.35	120.62	64.42	6.57	0.137
7	5.133	70.81	6.1613	3.6505	2.5108	242.98	116.49	129.00	13.15	0.186
8	4.361	43.43	4.5795	1.8845	2.6950	192.90	122.54	73.05	7.45	0.171
9	4.460	46.45	8.6985	6.1946	2.5039	202.68	113.77	91.41	9.32	0.201
10	4.710	54.71	10.1146	7.8077	2.3069	251.08	132.79	120.60	12.29	0.225
11	4.821	58.67	6.6473	3.7740	2.8734	212.65	112.77	102.76	10.48	0.179

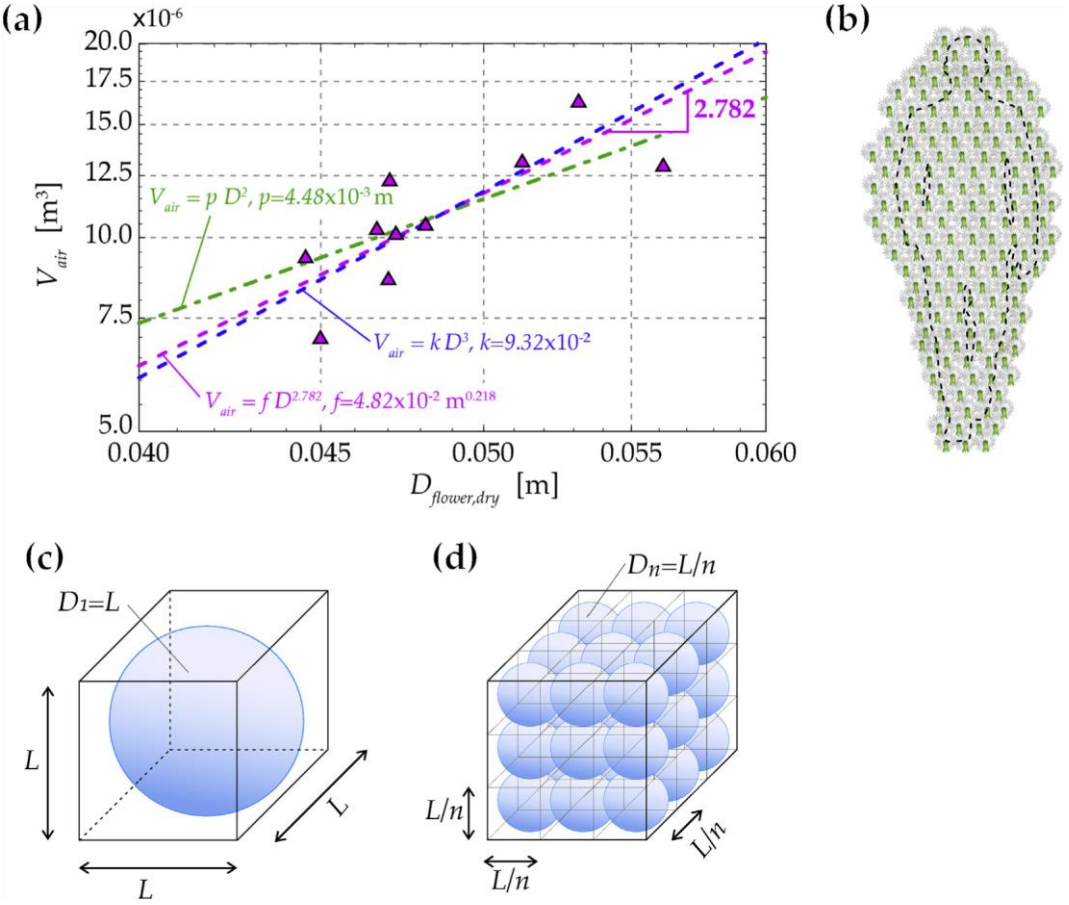

Fig. 5. (a) Log-log plot of the volume of the trapped air within the seed head. The results are best fitted with a scaling law characterized by a fractal exponent of 2.782 and a fractal air entrapped volumetric content of 4.82 10^2 $m^{0.218}$ (purple/dashed line). The classical Euclidean scaling law with a dimension of 3 (blue/dashed line) and the scaling low with dimension 2 (dashed-dotted/green line) are also reported for comparison. (b) A human body covered with about 360 Dandelion seed heads (180 seed-head/m^2) can survive 4¯8 min (air consumption of 5¯10 l/min) in apnea. (c,d) The optimal design, for the same volume, is attained increasing the number of small elements rather than using larger elements in a lower number. (c) The same volume is filled with just 1 seed head (diameter D_1 ¼ L) and (d) with n^3 smaller seed heads of diameter D_n ¼ L/n (3D splitting). (d) The same area L L is covered with n^2 smaller seed heads (2D splitting). In the figure n ¼ 3.

where y_i represents each data points, y_{fit} the regression value provided by the fitting law and m the number of data points. We calculated the RMSE for the three fitting laws reported in Fig. 5, namely with exponents α equal to 2 (a bad fit), 2.782 (the best fit) and 3 (a good fit). The lower the error in the regression analysis relative to total error; the lower the RMSE value will be, with a best value RMSE ¼ 0 for a perfect fit. From the analysis, we estimated an RMSE ffi 1:70 mm^3 for the best fit (exponent 2.782), RMSE ffi 1:75 mm^3 for the good fit (exponent 3), and RMSE ffi 1:78 mm^3 for the bad fit (exponent 2).

4. Example of a potential technological application of the dandelion air(gas)-trapping mechanisms: underwater life vest

This section is devoted to providing some insights into the potential technological applications of the Dandelion air(gas)-trapping mechanism towards the realization of bioinspired devices.

Thinking about the engineering of a Dandelion-like material, it is convenient to consider the case of a self-similar splitting over the surface (2D splitting) rather than in the volume (3D splitting), as shown in Fig. 5(e). This different scaling can be obtained imagining the number of layers N independent from the diameter of the n n seed heads over the surface. In this case, eq. (9) modifies in:

$V_n^{\delta};_{2airD\ splitting}{}^{p}$ ¼ $Nn_{2\alpha}$: (11)

$V_{1;air}$

From eqs. (8) and (11) the optimal design, i.e. optimal size and required number of layers N, can be derived.

For the sake of illustration, we consider the example reported in Fig. 5(b), where N layers of miniaturized seed heads covers a human body. The seed heads have the optimal diameter provided by eq. (8) and thus equal to about 18 μm. Each seed head can retain approximatively 3.44 10^{12} l of air. The volume of the air retained by a surface of 1 m^2 (containing more or less 5 10^9 seed heads) is about 0.015 l/m^2. Thus, a human body (surface area of about 2 m^2) could remain in apnea

(air consumption of 5¯10 l/min) for 10 min if covered with a Dandelion-like material made up of ¯ Nffi1700¯3400 layers of such seed heads with a total thickness of ffi3 6 cm.

The described mechanism could be also exploited to create an innovative bioinspired bubble-trap device capable to avoid gas nucleation [42,43] and safely guiding away dangerous gases bubbles that, changing their intrinsic physical properties, could lead to serious problems in fluidic/microfluidic systems.

The fractal nature of the volume of the trapped air plays a crucial role in the design of bioinspired devices, e.g. the realization of a prototype made up of artificial Dandelion flowers. In particular, a scaling law with a characteristic dimension lower than 3 ¯ as expected and observed ¯ implies that the percentage of the entrapped volume of air is not constant but depends on the nominal size of the flower. Essentially, an exponent lower than 3 suggests that a miniaturization of Dandelion-like components leads to an increase in the efficiency of the air encapsulation that has thus to be maximized increasing the number of layers of small elements rather than using larger elements in lower number of layers. This scaling would be absent for an exponent equal to 3 that is the nominal thus Euclidean value, in spite of the similar fit compared in Fig. 5.

Conclusions

In this article, we have reported the observation of an interesting airencapsulating elastic mechanism of Dandelion seed heads when submerged under water. The scaling of the volume of the air entrapped suggests its fractal nature with a dimension of 2.782 and a fractal air volume fraction of 4.82 10–^{2} m$^{0.218}$, resulting in nominal air volume fractions in the range of 14 23% with a mean value of 0:185 0:026 corresponding to a buoyant force of 105:043 28:22 mN. We have shown that the fractal nature of the seed heads suggests that the miniaturization of Dandelion-like components leads to an increase in the efficiency of the resultant bioinspired material for 3D or 2D splittings. Moreover, an optimal size for simultaneously maximizing efficiency and reducing material/weight/cost emerges of about 18 μm. This interesting air-retaining mechanism paves the wave toward the realization of innovative biomimetic devices and new related technological solutions for conveying air-bubbles under water.

Author contribution

Maria Consolata Pugno discovered the phenomenon, Diego Misseroni performed the experiments, Diego Misseroni and Nicola M. Pugno developed the analytical approach and wrote the article.

Declaration of competing interest

The authors declare that they have no known competing financial interests or personal relationships that could have appeared to influence the work reported in this paper.

Acknowledgments

N.M.P. and D.M. are supported by the European Commission under the FET Open (Boheme) grant No. 863179, as well as by the Italian Ministry of Education, University and Research (MIUR) under the 'Departments of Excellence' grant L. 232/2016. The authors thank Mr. F. Vinante for assistance during the experiments.

Appendix A. Supplementary data

Supplementary data to this article can be found online at https:// doi.org/10.1016/j.mtbio.2021.100095.

References

[1] Eugene C. Goldfield, Bioinspired Devices. Emulating Nature's Assembly and Repair Process, Harvard University Press, 2018.
[2] B. Mazzolai, et al., Octopus-Inspired soft arm with suction cups for enhanced grasping tasks in confined environments, Adv. Intell. Syst. 1 (6) (2019) 1900041.
[3] S. Kim, C. Laschi, B. Trimmer, Soft robotics: a bioinspired evolution in robotics, Trends Biotechnol. 31 (5) (2013) 287¯294.
[4] L. Cen, A. Erturk, Bio-inspired aquatic robotics by untethered piezohydroelastic actuation, Bioinspiration Biomimetics 8 (1) (2013), 016006.
[5] D. Floryan, T. Van Buren, A.J. Smits, Efficient cruising for swimming and flying animals is dictated by fluid drag, Proc. Natl. Acad. Sci. U.S.A. 115 (32) (2018) 8116¯8118.
[6] Ahmad Rafsanjani, et al., Kirigami skins make a simple soft actuator crawl, Sci. Robot. 3 (2018) 7555.
[7] F. Dal Corso, et al., Serpentine locomotion through elastic energy release, J. R. Soc. Interface 14 (130) (2017) 20170055.
[8] D. Bigoni, et al., Torsional locomotion, Proc. R. Soc. A 470 (2014) 20140599.
[9] Ali Sadeghi, et al., A plant-inspired robot with soft differential bending capabilities, Bioinspiration Biomimetics 12 (2016), 015001.
[10] B. Chen, P.D. Wu, H. Gao, Hierarchical modelling of attachment and detachment mechanisms of gecko toe adhesion, Proc. R. Soc. A 464 (2094) (2008) 1639¯1652.
[11] A. Bührig-Polaczek, et al., Biomimetic cellular metals using hierarchical structuring for energy absorption, Bioinspiration Biomimetics 11 (2016), 045002.
[12] G. Greco, et al., The role of hairs in the adhesion of octopus suckers: a hierarchical peeling approach, Bioinspiration Biomimetics 15 (2020), 035006.
[13] N.M. Pugno, E. Lepore, Observation of optimal gecko's adhesion on nanorough surfaces, Biosystems 94 (3) (2008) 218¯222.
[14] E. Lepore, A. Chiodoni, N. Pugno, New topological and statistical observations on the moult and skin of tokay geckos, Rev. Adv. Mater. Sci. 24 (2010) 69¯80.
[15] K. Autumn, N. Gravish, Gecko adhesion: evolutionary nanotechnology, Philos. Trans. R. Soc. A 366 (1870) (2008) 1575¯1590.
[16] W. Barthlott, C. Neinhuis, Purity of the sacred lotus, or escape from contamination in biological surfaces, Planta 202 (1) (1997) 1¯8.
[17] A. Solga, et al., The dream of staying clean: Lotus and biomimetic surfaces, Bioinspiration Biomimetics 2 (4) (2007) S126.

[18] E. Lepore, N.M. Pugno, Superhydrophobic polystyrene by direct copy of a lotus leaf, BioNanoScience 1 (4) (2011) 136–143.

[19] K.Y. Law, Definitions for Hydrophilicity, Hydrophobicity, and Superhydrophobicity: Getting the Basics Right, ACS Publication, 2014, pp. 686–688. [20] A. Antony, G. Leslie, Degradation of Polymeric Membranes in Water and Wastewater Treatment, in: Advanced Membrane Science and Technology for Sustainable Energy and Environmental Applications, Woodhead Publishing, 2011, pp. 718–745.

[21] R.S. Seymour, P.G. Matthews, Physical gills in diving insects and spiders: theory and experiment, J. Exp. Biol. 216 (2) (2013) 164–170.

[22] H.W. Levi, Adaptations of respiratory systems of spiders, Evolution 21 (1967) 571–583.

[23] R.S. Seymour, S.K. Hetz, The diving bell and the spider: the physical gill of Argyroneta aquatica, J. Exp. Biol. 214 (13) (2011) 2175–2181.

[24] D. Woermann, On the mechanical stability of the air volume trapped within the diving bell of the water spider Argyroneta aquatica (Araneae; Cybaeidae); a thermodynamic analysis based on a model, Belg. J. Zool. 140 (2010) 244–248.

[25] W. Barthlott, et al., The Salvinia paradox: superhydrophobic surfaces with hydrophilic pins for air retention under water, Adv. Mater. 22 (2010) 2325–2328.

[26] M. Amabili, et al., Unraveling the Salvinia paradox: design principles for submerged superhydrophobicity, Adv. Mater. Interfaces 2 (2015).

[27] P. Ditsche, et al., Elasticity of the hair cover in air-retaining Salvinia surfaces, Appl. Phys. 121 (2015) 505–511.

[28] Matthias J. Mayser, et al., Measuring air layer volumes retained by submerged floating-ferns Salvinia and biomimetic superhydrophobic surfaces, Beilstein J. Nanotechnol. 5 (2014) 812–821.

[29] O. Tricinci, et al., Air trapping mechanism in artificial Salvinia-like micro-hairs fabricated via direct laser lithography, Micromachines 8 (2017) 366.

[30] O. Tricinci, et al., 3D micropatterned surface inspired by Salvinia molesta via direct laser lithography, ACS Appl. Mater. Interfaces 7 (46) (2015) 25560–25567.

[31] M.N. Kavalenka, et al., Bioinspired air-retaining nanofur for drag reduction, ACS Appl. Mater. Interfaces 7 (2015) 10651–10655.

[32] D. Zheng, et al., "Salvinia-effect-inspired "sticky" superhydrophobic surfaces by meniscus-confined electrodeposition", Langmuir 33 (47) (2017) 13640–13648.

[33] Y. Xiang, et al., Superrepellency of underwater hierarchical structures on Salvinia leaf, Proc. Natl. Acad. Sci. U.S.A. (1) (2020) 2282–2287.

[34] M. Mail, et al., "Air retaining grids—a novel technology to maintain stable air layers under water for drag reduction", Philos. Trans. R. Soc. A 377 (2150) (2019) 20190126.

[35] Y. Yang, J. Busch, et al., Bionics and green technology in maritime shipping: an assessment of the effect of Salvinia air-layer hull coatings for drag and fuel reduction, Philos. Trans. R. Soc. A 377 (2138) (2019), 20180263.

[36] J. Hunt, B. Bhushan, Nanoscale biomimetics studies of Salvinia molesta for micropattern fabrication, J. Colloid Interface Sci. 363 (1) (2011) 187–192.

[37] D.J. Babu, et al., Superhydrophobic vertically aligned carbon nanotubes for biomimetic air retention under water (Salvinia effect), Adv. Mater. Interfaces 4 (13) (2017) 1700273.

[38] C. Cummins, et al., A separated vortex ring underlies the flight of the dandelion, Nature 562 (2018) 414.

[39] F. Bosi, et al., "Self-encapsulation, or the 'dripping' of an elastic rod, Proc. R. Soc. A 471 (2015) 20150195.

[40] H. Elettro, et al., "In-drop capillary spooling of spider capture thread inspires hybrid fibers with mixed solid–liquid mechanical properties, Proc. Natl. Acad. Sci. U.S.A. 113 (2016) 6143–6147.

[41] S. Neukirch, A. Antkowiak, J.J. Marigo, The bending of an elastic beam by a liquid drop: a variational approach, Proc. R. Soc. A 469 (2013) 20130066.

[42] H. de Maleprade, M. Pautard, C. Clanet, D. Quere, Tightrope bubbles, Appl. Phys. Lett. 114 (23) (2019) 233704.

[43] I. Pereiro, A.F. Khartchenko, L. Petrini, G.V. Kaigala, Nip the bubble in the bud: a guide to avoid gas nucleation in microfluidics, Lab Chip 19 (14) (2019) 2296–2314.